Note on the sample for a massless scalar iso-curvature system

A. Initial condition and parameter settings

Here we consider the iso-curvature perturbation generated by a massless scalar field ϕ. We assume that the massless scalar field does not contribute to the background metric of the gradient expansion. Then, as is described in Ref. [1], once the spatial profile $\Upsilon(\boldsymbol{x})$ of the scalar field is specified at the leading order of the gradient expansion, the growing mode solution can be described up through the next-to-leading order of the long-wavelength approximation. We use the analytic expressions for the geometrical variables with the constant-mean-curvature and zero-shift gauge up through the next-to-leading order as the initial data for the sample code.

In this sample code, we consider the numerical domain given by $-L \leq X \leq L$, $0 \leq Y \leq L$ and $0 \leq Z \leq L$ with X, Y and Z being the reference Cartesian coordinates. The specific profile of Υ is the same as in Ref. [1]:

$$\Upsilon = \mu \exp\left(-\frac{1}{6}k^2R^2\right) W(R), \tag{1}$$

where $R^2 = X^2 + Y^2 + Z^2$ and the function $W(R)$ is given by [2]

$$W(R; R_{\rm W}, L) = \begin{cases} 1 & \text{for } 0 \leq R \leq R_{\rm W} \\ 1 - \frac{\left((R_{\rm W}-L)^6 - (L-R)^6\right)^6}{(R_{\rm W}-L)^{36}} & \text{for } R_{\rm W} \leq R \leq L \\ 0 & \text{for } L \leq R \end{cases} \tag{2}$$

with $R_{\rm W} = 0.8L$. The parameters k and μ are set as $k = 10/L$ and $\mu = 0.65$. The amplitude μ is slightly larger than the threshold value $\mu_{\rm th} \simeq 0.63$ for PBH formation reported in Ref. [3].

The background universe is assumed to be radiation-dominated, and the Hubble parameter at the initial time $H_{\rm i}$ is set to be $H_{\rm i} = 50/L$. The coordinate length L is covered by 36 grid points with grids on both ends. Since this sample code is just for demonstration, we do not seriously consider the constraint violations.

B. Non-Cartesian coordinate

In this sample code, we employ the non-Cartesian coordinate system (x, y, z) firstly implemented in Ref. [2]. The non-Cartesian coordinates x^i are related to the Cartesian coordinates X^i as follows:

$$X^i = x^i - \frac{\eta}{1+\eta}\frac{L}{\pi}\sin\left(\frac{\pi}{L}x^i\right). \tag{3}$$

This functional form is compatible with the boundary conditions adopted in this sample code (see Fig. 1. and Ref. [4]) and satisfies $x^i = 0$ at $X^i = 0$ and $x^i = L$ at $X^i = L$.

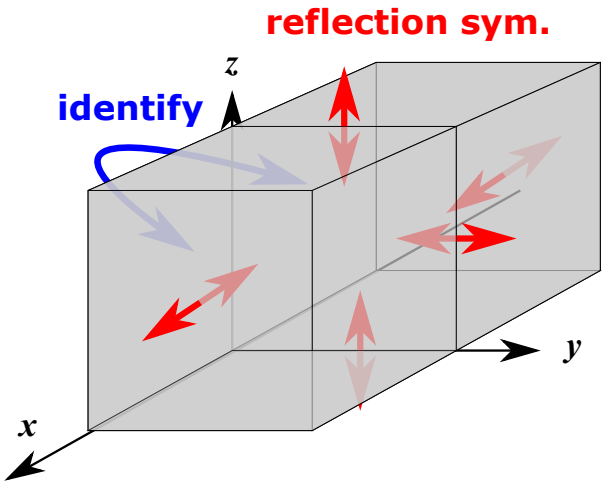

FIG. 1: The numerical region and boundary conditions.

At the origin, the infinitesimal interval in the Cartesian coordinate ΔX is covered by the non-Cartesian coordinate interval $\Delta x = (1+\eta)\Delta X$. Therefore the central part is enlarged in this non-Cartesian coordinate system. In this sample code, the value of η is set to 10.

C. Mesh refinement

On top of the non-Cartesian coordinate system, we implement fixed mesh refinement. We do not explain the details of our mesh refinement procedure but attach a simple schematic diagram showing our procedure (Fig. 2). In the sample code, 2 additional layers for the mesh refinement are introduced when the value of the lapse function at the origin reduces to 0.3 and 0.15. The region covered by one higher layer is the region covered by 9 grids in the lower layer. These parameters for the mesh refinement can be controlled by the parameter file `par_fmr.d`.

D. Results of the time evolution

In the default setting, the time evolution starts from the data given by the data file `ini_all.dat`, which describes the system soon after the horizon formation. When the numerical code is executed, first the data file `ini_all.dat`, in which 2 higher layers are already introduced, is loaded. Then the apparent horizon finder starts and a horizon will be found after some time (see Fig. 3). The time evolution starts after the apparent horizon finder. After 3 steps of the evolution, all the data will be restored into `out_all.dat`, and the calculation stops. The value of the lapse function on the x-y plane is depicted in Fig. 4. The value of the scalar field ϕ on the x-y plane is depicted in Fig. 5. We see that the scalar field configuration is sharply peaked at the origin and the resolution is not sufficient to resolve

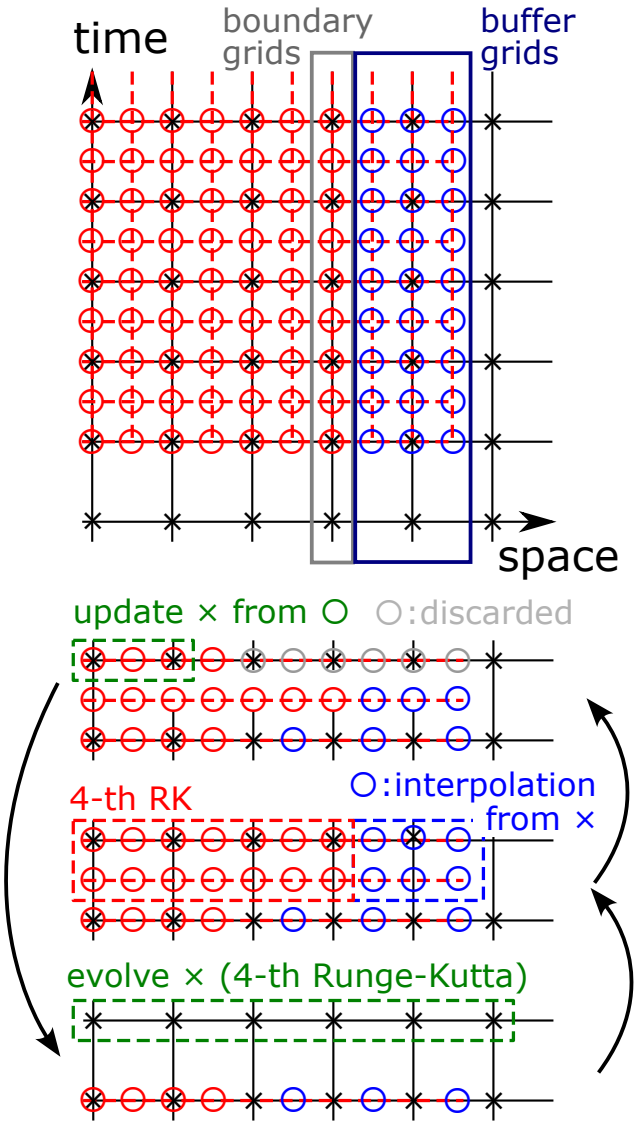

FIG. 2: The mesh refinement procedure.

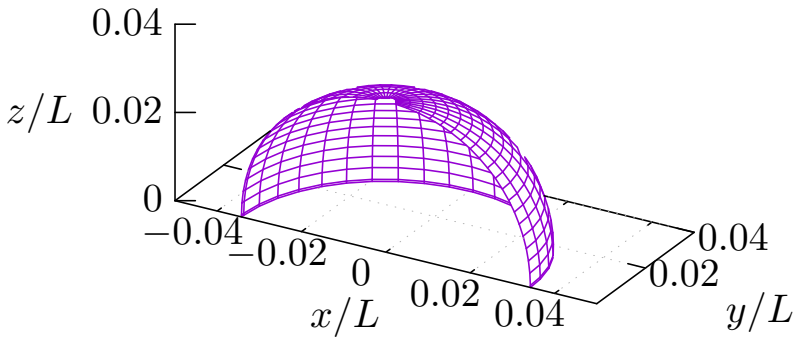

FIG. 3: Figure of the apparent horizon generated from `out_AHfig.dat`.

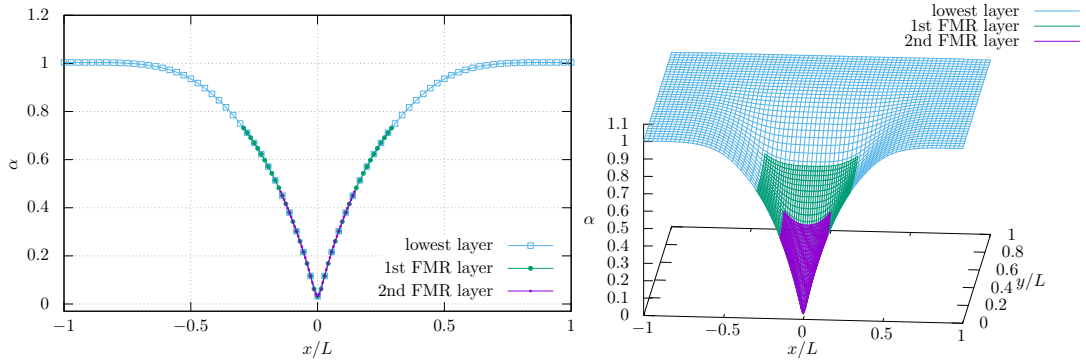

FIG. 4: Lapse function on the x-axis generated from 1st and 2nd columns in `out_xkl.dat` (left) and $x-y$ plane generated from 1st, 2nd and 3rd columns in `out_xyl.dat` (right).

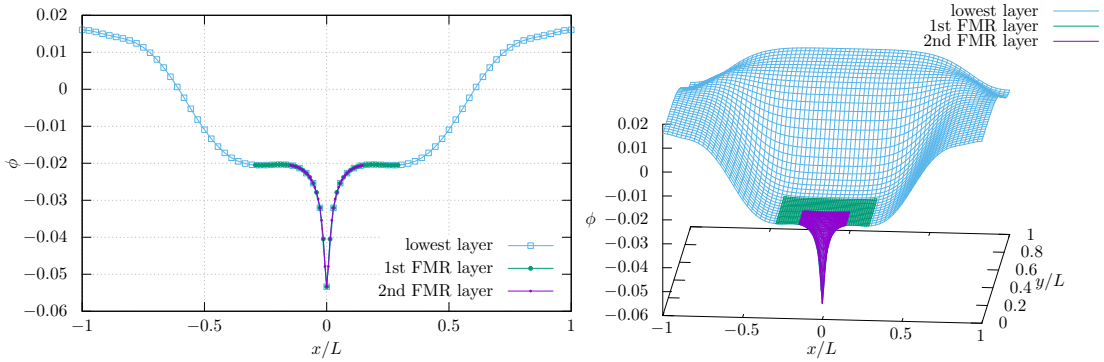

FIG. 5: The scalar field ϕ on the x-axis generated from 1st and 48th columns in `out_xkl.dat` (left) and $x-y$ plane generated from 1st, 2nd and 49th columns in `out_xyl.dat` (right).

the scalar field profile near the origin.

To start the time evolution from the initial data described in the previous sections, One has to set the value of "*maximum step of the main loop*" in `par_ini.d` to a sufficiently large number and set the value of the line indicated by "*0:no continue 1:continue*" to 0. Then one finds PBH formation at around the coordinate time $t \simeq 20.1L$. It takes a very long time.

E. Excision

When an apparent horizon is found, the excision prescription is introduced. We follow the procedure given in Ref. [5]. The region excised is a cubic region whose size can be

controlled by the parameter "*excision grid*" in `par_ini.d`.

---

[1] C.-M. Yoo, T. Harada, S. Hirano, H. Okawa, and M. Sasaki, Phys. Rev. D **105**, 103538 (2022), arXiv:2112.12335, *Primordial black hole formation from massless scalar isocurvature.*

[2] C.-M. Yoo, T. Ikeda, and H. Okawa, Class. Quant. Grav. **36**, 075004 (2019), arXiv:1811.00762, *Gravitational Collapse of a Massless Scalar Field in a Periodic Box.*

[3] C.-M. Yoo, T. Harada, and H. Okawa, Phys. Rev. D **102**, 043526 (2020), arXiv:2004.01042, *Threshold of Primordial Black Hole Formation in Nonspherical Collapse*, [Erratum: Phys.Rev.D 107, 049901 (2023)].

[4] C.-M. Yoo, Phys. Rev. D **110**, 043526 (2024), arXiv:2403.11147, *Primordial black hole formation from a nonspherical density profile with a misaligned deformation tensor.*

[5] M. Alcubierre and B. Bruegmann, Phys. Rev. D **63**, 104006 (2001), arXiv:gr-qc/0008067, *Simple excision of a black hole in (3+1)-numerical relativity.*